



ELSEVIER

Available online at www.sciencedirect.com

SCIENCE @ DIRECT®

Optics Communications 226 (2003) 337–344

OPTICS
COMMUNICATIONS

www.elsevier.com/locate/optcom

Numerical modeling of CW-pumped repetitively passively Q-switched Yb:YAG lasers with Cr:YAG as saturable absorber

Jun Dong *

School of Optics and Center for Research and Education in Optics and Lasers (CREOL), University of Central Florida, Orlando, FL 32816-2700, USA

Received 29 May 2003; accepted 4 September 2003

Abstract

Passively Q-switched Yb:YAG lasers with Cr⁴⁺:YAG as saturable absorber is numerically studied by solving the coupled rate equations. The stimulation results indicate that the results obtained numerically are in good agreement with those obtained experimentally. From the stimulation results, the parameters (reflectivity of the output coupler, the concentration of the saturable absorber, etc.) for the best Q-switched operation can be obtained. And the effect of pump power on the laser performance of passively Q-switched Yb:YAG lasers were studied systematically and results show that the good laser performance can be achieved by higher pump power. A typical passively Q-switched laser pulse of 0.49 mJ with 32 ns in width at the repetition rate of 17 kHz can be obtained with a typical laser configuration, which results in 15.3 kW peak power.

© 2003 Elsevier B.V. All rights reserved.

PACS: 42.55.Xi; 42.60.Gd; 02.60.Cb

Keywords: Q-switched laser; Yb:YAG; Saturable absorber; Numerical stimulation

1. Introduction

Laser diode (LD) pumped passively Q-switched solid-state lasers are currently explored extensively and used as miniature or micro-lasers capable of delivering high peak power (~kW to MW) at high

repetition rates and short nanosecond (ns) or sub-nanosecond pulse width. These lasers can be potentially used in micromachining, remote sensing, target ranging, and microsurgery, etc. Most of the work on passively Q-switched microchip lasers has concentrated on laser diode pumped Nd lasers with a Cr⁴⁺:YAG as saturable absorber [1,2]. In recent years, passively Q-switched Yb:YAG lasers using Cr⁴⁺:YAG as saturable absorber have been reported [3,4]. Compared to Nd ions in laser crystals, Yb ion is ideally suited for diode pumping

* Tel.: +14078235009; fax: +14078236880.

E-mail address: jundong@mail.ucf.edu.

since it has a very simple energy level scheme with desirable properties for a laser system. Furthermore, diode pumped Yb:YAG lasers have several advantages relative to Nd:YAG lasers, such as a long storage lifetime (951 μs) [5] which is suitable for storing energy and Q-switching operation, a very low quantum defect (8.6%), resulting in three times less heat generation during lasing than comparable Nd-based laser systems [6], large absorption width around the InGaAs laser emission range [7], a relatively large emission cross-section, easy growth of high quality and moderate concentration crystal without concentration quenching, and strong energy-storing capacity. Another advantage of using Yb:YAG is that the 940-nm absorption feature is approximately 18 times broader than the 808 nm absorption feature in Nd:YAG and therefore the Yb:YAG system is less sensitive to diode wavelength specifications [8]. Q-switched operation of Yb:YAG lasers by using the electro-optic switch [9] and semiconductor saturable absorber mirror (SESAM) [10] were also reported. Dong et al. [3] first reported passively Q-switched Yb:YAG laser with Cr^{4+} :YAG as saturable absorber and obtained 3.2 μJ /pulse output energy with pulse width of 350 ns at 17 kHz repetition rate. Kalisky et al. [4] reported laser diode pumped passively Q-switched Yb:YAG lasers with Cr^{4+} -doped garnets as saturable absorber, and obtained about 0.5 mJ/pulse output energy with pulse width of about 48 ns, resulting peak power around 10.4 kW.

There are a number of publications dealing with modeling of passively Q-switched Nd^{3+} lasers with Cr^{4+} as saturable absorber [11–15], for simplicity, in their analysis of the output pulse characteristics (pulse energy, peak power and pulse width), they ignore the pump power effects on the output pulse characteristics. In real life, the Q-switched laser pulse characteristics are varied with the pump power. To more accurately simulate the behavior of the passively Q-switched laser pulse, the pump power term should be included in the rate equation, the actual solution to the Q-switched rate equations can be achieved by solving the rate equations numerically. In this paper, the optical performance of the passively Q-switched Yb:YAG laser with Cr^{4+} :YAG as saturable absorber was

theoretically investigated by solving the coupled rate equations, and effects of pump rate, reflectivity of the output coupler, the concentration of the saturable absorber and the laser cavity length on the performance of passively Q-switched Yb:YAG laser with Cr^{4+} :YAG as saturable absorber are addressed.

2. Passively Q-switching theory

According to the passively Q-switched theory [11,13,14], the modified coupled rate equations of photon density and population inversion density of gain medium and the saturable absorber in the passively Q-switched resonator, which includes the excited-state absorption of the saturable absorber, the pump term and the population reduction factor of the laser, are as follows:

$$\frac{d\phi}{dt} = \frac{\phi}{t_r} \left(2\sigma N l - 2\sigma_g N_g l_s - 2\sigma_e N_e l_s - \ln \left(\frac{1}{R} \right) - L \right), \quad (1)$$

$$\frac{dN}{dt} = -\gamma\sigma c\phi N - \frac{N}{\tau} + W_p, \quad (2)$$

$$\frac{dN_g}{dt} = -\sigma_g c\phi N_g + \frac{N_{s0} - N_g}{\tau_s}, \quad (3)$$

$$N_g + N_e = N_{s0}, \quad (4)$$

where ϕ is the photon density in the laser cavity of optical length l' , N is the population inversion density of the gain medium, σ is the stimulated emission cross-section of the laser crystal, t_r is the cavity round-trip time, $t_r = 2l'/c$, l is the length of the laser crystal, c is the speed of the light, σ_g is the absorption cross-section of ground state of the saturable absorber, σ_e is the absorption cross-section of the excited state, l_s is the length of the saturable absorber, N_g and N_e are the absorber ground state and excite state population density, respectively, N_{s0} is the total population density of the saturable absorber, R is the reflectivity of the output coupler, L is the nonsaturable intracavity round-trip dissipative optical loss, γ is the inversion reduction factor, $\gamma = 2$ for Yb^{3+} -doped three-level solid state lasers, W_p is the volumetric

pump rate into the upper laser level and is proportional to the CW pump power, τ is the lifetime of the upper laser level of the gain medium, τ_s is the excited-state lifetime of the saturable absorber.

Because the buildup time of the Q-switched laser pulse is generally quite short compared with the pumping and relaxation times of the gain medium, it is reasonable to neglect the effect of pumping and spontaneous decay of the laser population inversion density during pulse generation, with this assumption, Eq. (2) becomes,

$$\frac{dN}{dt} \cong -\gamma\sigma c\phi N. \tag{5}$$

When the photon intensity is low, almost all the population of the saturable absorber is in the ground state, hence we can approximate the initial population inversion density before saturation of the saturable absorber by setting the right-hand side of Eq. (1) to zero and assume that $N_g = N_{s0}$, so initial population inversion density can be written as,

$$N_i = \frac{2\sigma_g N_{s0} l_s + \ln(1/R) + L}{2\sigma l}. \tag{6}$$

When the photon intensity is high, most of the population in the ground state of the saturable absorber is excited to the excited state. Therefore, we can approximate the population inversion density after the bleaching of the saturable absorber by setting right hand side of Eq. (1) to zero and assuming that $N_g \cong 0$, the threshold population inversion density can be written as,

$$N_{th} \cong \frac{2\sigma_e N_{s0} l_s + \ln(1/R) + L}{2\sigma l}. \tag{7}$$

With expression (7) we can rewrite Eq. (1) as

$$\frac{d\phi}{dt} = \frac{\phi}{t_r} (2\sigma N l - 2\sigma N_{th} l). \tag{8}$$

Dividing expression (8) by expression (5) gives,

$$\frac{d\phi}{dN} = -\frac{l}{l'} \frac{N - N_{th}}{\gamma N}. \tag{9}$$

Eq. (9) can be integrated from the time of Q-switch opening to an arbitrary time t as follows:

$$\int_{\phi_i}^{\phi(t)} d\phi = -\frac{l}{l'\gamma} \int_{N_i}^{N(t)} \left(1 - \frac{N_{th}}{N}\right) dN. \tag{10}$$

Initial photon density ϕ_i is small compared with the value of ϕ anytime during the laser output pulse. Hence the solution of expression (10) is

$$\phi(t) \cong \frac{l}{l'\gamma} \left[N_i - N - N_{th} \ln \left(\frac{N_i}{N} \right) \right]. \tag{11}$$

As can be inferred from expression (8), the photon number reaches a peak value ϕ_{peak} when N is equivalent to N_{th} . Hence from expression (11), we have

$$\begin{aligned} \phi_{peak} &\cong \frac{l}{l'\gamma} \left[N_i - N_{th} - N_{th} \ln \left(\frac{N_i}{N_{th}} \right) \right] \\ &= \frac{lN_i}{l'\gamma} \left[\frac{N_i/N_{th} - 1 - \ln(N_i/N_{th})}{N_i/N_{th}} \right]. \end{aligned} \tag{12}$$

Expression (12) indicates that, when N_i/N_{th} approaches to infinity, the peak photon number approaches the maximum available population inversion density $lN_i/l'\gamma$.

After the release of the Q-switched laser pulse, laser population inversion density N is depleted by the photon flux and is reduced to a value below N_{th} . We can derive this final population inversion density N_f from expression (11) by setting $\phi \cong 0$ because the photon density is small after the release of the Q-switched laser pulse. Let $N = N_f$ and $\phi = 0$ then expression (11) becomes,

$$N_i - N_f - N_{th} \ln \left(\frac{N_i}{N_f} \right) = 0. \tag{13}$$

Expression (13) is transcendental and can be solved numerically. When N_i and N_f are known, the output pulse energy E , peak power P and pulse width τ_p of passively Q-switched Yb:YAG laser can be written as [16]:

$$E = \frac{h\nu A}{2\sigma\gamma} \ln \left(\frac{1}{R} \right) \ln \left(\frac{N_i}{N_f} \right), \tag{14}$$

$$P = \frac{h\nu A l}{\gamma t_r} \ln \left(\frac{1}{R} \right) \left[N_i - N_{th} - N_{th} \ln \left(\frac{N_i}{N_{th}} \right) \right], \tag{15}$$

$$\tau_p \approx \frac{E}{P}, \quad (16)$$

where $h\nu$ is the photon energy, A is the active area of the beam in the laser medium.

Expression (11)–(16) may be used to quantitatively evaluate the optical performance of a laser that is passively Q-switched with a slow-relaxing saturable absorber without actually executing the numerical calculation. N_i , N_{th} , N_f are the population inversion densities at the start of Q-switching, the point of maximum power and the end of the Q-switched pulse, respectively.

With continuous-wave pumping, the laser will passively Q-switched as soon as the gain exceeds the combined saturable and unsaturable losses in the resonator. As the incident pump power is increased, the laser eventually reaches a threshold condition and begins to repetitively Q-switched with a time interval between pulses, t_c . The pulse energy and pulse repetition rate will be increased and the pulse width will be decreased with further increasing of the incident pump power.

For continuous-wave pumped repetitive Q-switching laser at a repetition rate f , the maximum time available for the inversion to build up between pulses is $t_c = 1/f$. Therefore, the initial inversion density of the Q-switch under the influence of the absorbed pump power can be written as [17]:

$$N_i = N_{cw} - (N_{cw} - N_f) \exp\left(\frac{-1}{\tau f}\right) \quad (17)$$

in order to have the inversion return to its original value after each Q-switch cycle, where N_{cw} is the continuous-wave pumping inversion density inside the resonator, $N_{cw} = W_p \tau$, W_p is the volumetric pump rate into the upper laser level and is proportional to the continuous-wave pump power, $W_p = (P_p[1 - \exp(-2\alpha l)])/(h\nu_p A_p l)$, P_p is the incident pump power, $h\nu_p$ is the pump photon energy, A_p is the pump beam area, α is the absorption coefficient of gain medium at pump wavelength, l is the length of the gain medium. Eqs. (17) and (13) can be solved numerically to obtain the initial inversion density, N_i and final inversion density, N_f for continuous-wave pumped repetitively Q-switched lasers.

3. Numerical stimulation

The spectral parameters of Yb:YAG and Cr⁴⁺:YAG used for numerical stimulation of Cr⁴⁺:YAG passively Q-switched Yb:YAG laser are taken from [3,4] and listed in Table 1. The ground state absorption cross-section of Cr⁴⁺:YAG ($3.2 \times 10^{-18} \text{ cm}^2$) is substantially greater than the emission cross-section of Yb:YAG ($2.3 \times 10^{-20} \text{ cm}^2$) at laser wavelength of 1.03 μm . Therefore, assuming that the effective laser beam area on the laser gain medium equal to that on the saturable absorber (this is reasonable for our case for Cr⁴⁺:YAG crystal is tightly bonded with Yb:YAG crystal), passively Q-switched Yb:YAG lasers using Cr⁴⁺:YAG as saturable absorber is satisfied with the second threshold condition [11]. In a previous work, we experimentally demonstrated Ti:sapphire laser pumped passively Q-switched Yb:YAG laser with a Cr⁴⁺:YAG as saturable absorber [3]. A single Q-switched laser pulse of 3.2 μJ in energy and 350 ns in duration at laser wavelength of 1.03 μm was obtained. The schematic diagram for the passively Q-switched Yb:YAG laser experiments is shown in Fig. 1(a), which consists of a 23-cm-long fold-shaped laser resonator with a flat output coupler of total reflectivity at 940 nm and an 97% reflectivity at laser wavelength of 1.03 μm .

According to Eq. (1), the loss of the Q-switched laser can be defined as

$$\text{Loss} \equiv \frac{2\sigma_g N_g l_s + 2\sigma_e N_e l_s + \ln\left(\frac{1}{R}\right) + L}{2\sigma l}. \quad (18)$$

Fig. 2 show the results of the numerical stimulation for the passively Q-switched Yb:YAG lasers

Table 1
The spectral parameters of Yb:YAG and Cr⁴⁺:YAG used in numerical simulations

σ_g	$3.2 \times 10^{-18} \text{ cm}^2$ [4]
σ_e	$4.5 \times 10^{-19} \text{ cm}^2$ [4]
σ	$2.3 \times 10^{-20} \text{ cm}^2$ [4]
τ	951 μs [3,4]
τ_s	3.4 μs
γ	2
$h\nu_p$	$2.112 \times 10^{-19} \text{ J}$
$h\nu$	$1.93 \times 10^{-19} \text{ J}$

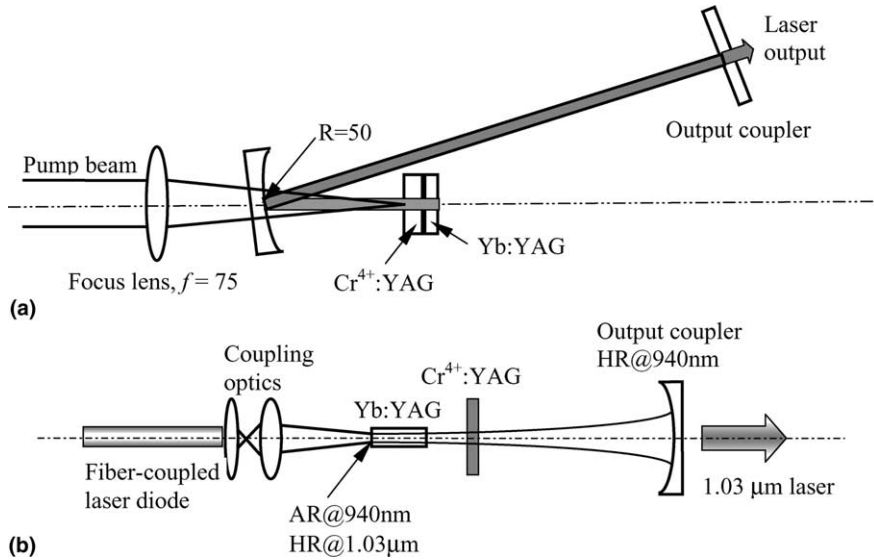


Fig. 1. Schematic diagrams of passively Q-switched Yb:YAG laser with Cr⁴⁺:YAG saturable absorber.

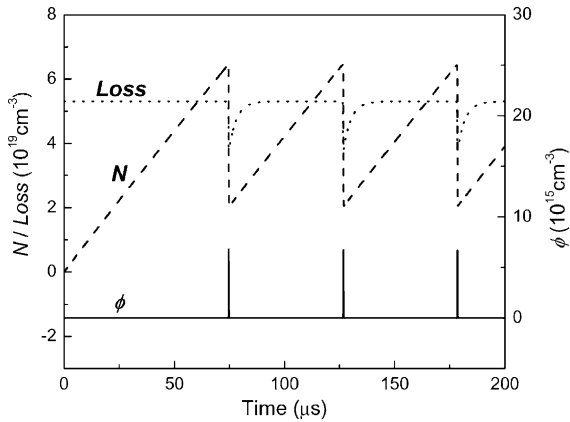


Fig. 2. Inversion density N , total loss of laser cavity, Loss and photon density, ϕ as functions of time.

with Cr⁴⁺:YAG as saturable absorber, obtained by solving Eqs. (1)–(3) with the Runge–Kutta method when pump rate $W_p = 9 \times 10^{23} \text{ s}^{-1} \text{ cm}^{-3}$ and the other parameters are as follows: $R = 97\%$, the intracavity loss is estimated to be 5%, the initial ground state population density, N_{s0} , is $4.5 \times 10^{16} \text{ cm}^{-3}$. It takes about 74 μs to develop the first Q-switched laser pulse, the time interval between subsequent Q-switched laser pulses is about 52 μs , which is shorter than that required for devel-

oping the first laser pulse because inversion density, N , does not decrease to zero after the release of the first laser pulse. The repetition rate can be estimated to be 19 kHz. Fig. 3 is an expanded picture of Fig. 2 near the occurrence of the first laser pulse. When the photon density inside the laser cavity increases, the loss decreases accordingly as a result of the bleaching effect of Cr⁴⁺:YAG saturable absorber. The photon density reaches its peak value when the laser inversion

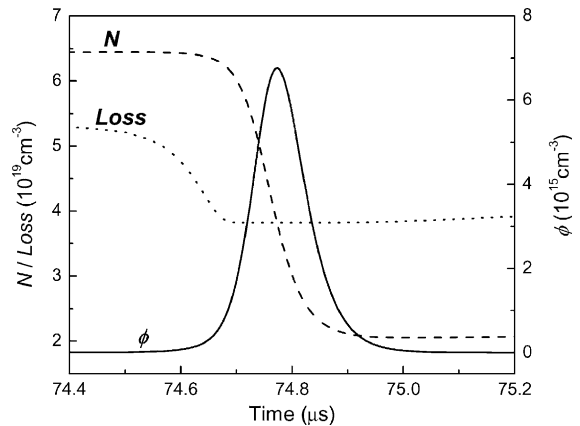


Fig. 3. Inversion density N , total loss of laser cavity, Loss and photon density, ϕ at the first Q-switched pulse as functions of time.

population equals to the cavity loss, i.e., when $N = \text{Loss} = 3.8 \times 10^{19} \text{ cm}^{-3}$, corresponding to the value calculated by Eq. (7). Beyond this point the laser inversion density (gain) is smaller than the total loss of the laser system, and the Q-switched laser pulse dies out quickly while the laser inversion population decreases gradually to a minimum value of $\sim 2.1 \times 10^{19} \text{ cm}^{-3}$. The increase of the loss after the release of the Q-switched laser pulse is due to the relaxation of the saturable absorber population. The initial laser inversion population required for laser action, $5.3 \times 10^{19} \text{ cm}^{-3}$, calculated with Eq. (6), is lower than that obtained by numerical simulation, $6.5 \times 10^{19} \text{ cm}^{-3}$. The cause of this difference is that we assume that $N = \text{Loss}$ in deriving the Eq. (6), whereas it is required that $N > \text{Loss}$ for the laser action to occur. From Fig. 3, the pulse width (full width at half-maximum) is about 248 ns, the output pulse energy (calculated by integration of the Q-switched laser pulse over a time range covering the entire laser pulse) is about $3.7 \mu\text{J}$, so the peak power can be determined to be 15 W.

The pump power has a great effect on the Q-switched laser performance, Fig. 4 shows the Q-switched Yb:YAG laser pulse energy, pulse width and repetition rate as functions of the pump rate, W_p , at $1.03 \mu\text{m}$ with reflectivity of output coupler, $R = 0.97$ and different concentrations of the saturable absorbers, N_{s0} . From Fig. 4(a), the Q-switched laser pulse energy increase with the pump rate for different concentration saturable absorber, the higher the concentration of saturable absorber (for the same length of the saturable absorber), and the higher pulse energy obtained. The pulse width decrease with the increase of pump rate for different concentration of saturable absorber, the higher the concentration of saturable absorber, the shorter the pulse width (as shown in Fig. 4(b)). At the lower pump rate near the pump threshold, the pulse width decreases dramatically (Fig. 4(b)) and pulse energy increase dramatically (Fig. 4(a)) with the pump rate. In the higher pump rate, the pulse energy increases slowly and pulse width decreases slowly with the pump rate. It is obvious that a better Q-switched laser performance can be achieved by using a high pumping rate, as expected from the theory.

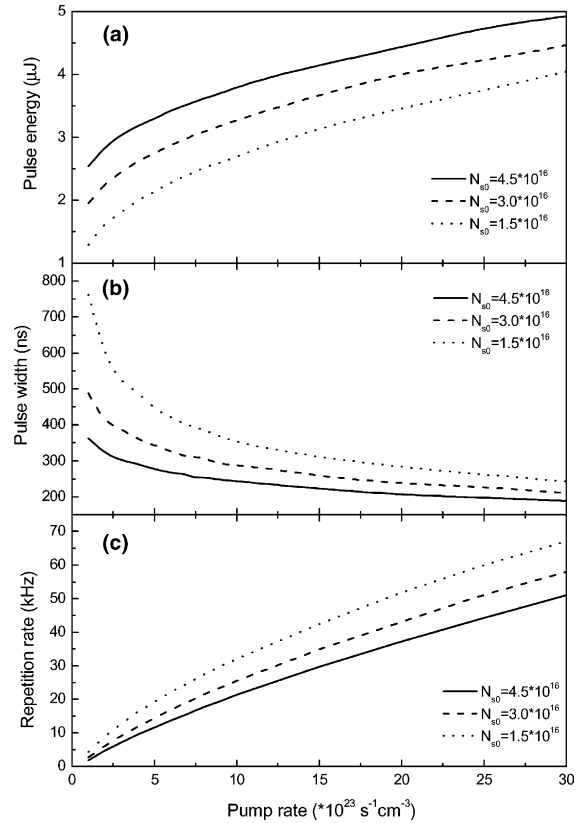


Fig. 4. The variation of Q-switched pulse energy, pulse width and repetition rate with pump rate for different concentrations of saturable absorber.

Fig. 4(c) shows that repetition rate increases nearly linearly with the pump rate, the higher the concentration of saturable absorber, the lower the repetition rate.

The reflectivity of output coupler also has great impact on the Q-switched laser characteristics, Fig. 5 shows the pulse energy, pulse width and repetition rate as a function of reflectivity of output coupler for different concentration of saturable absorber, the pump rate, $W_p = 9 \times 10^{23} \text{ s}^{-1} \text{ cm}^{-3}$, and the other parameters remain the same. The Q-switched pulse energy increases and the pulse width decreases for a specific reflectivity of output coupler when the concentration of saturable absorber increases. The results show that a better passively Q-switched Yb:YAG laser performance with Cr^{4+} :YAG as saturable absorber, such as a short pulse width and a high pulse energy output,

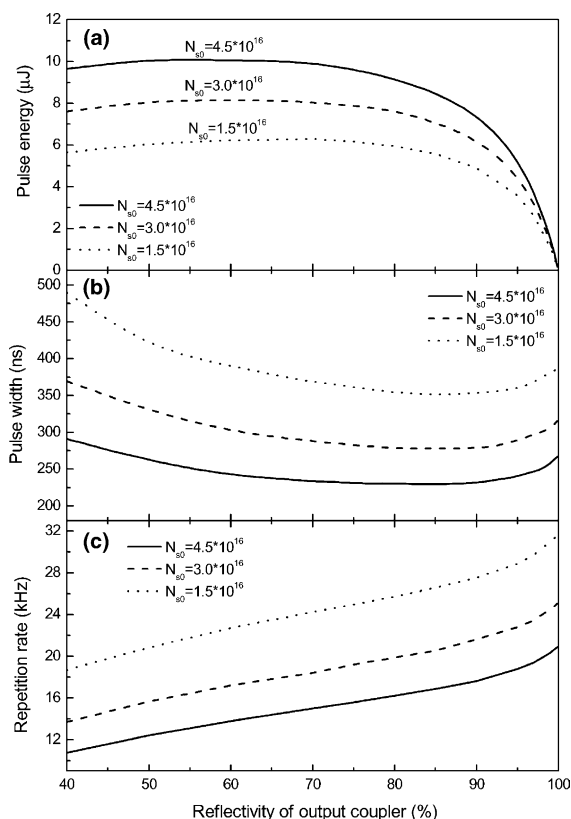


Fig. 5. The Q-switched pulse energy, pulse width and repetition rate as a function of reflectivity of the output coupler for different concentrations of the saturable absorber.

can be realized by using a thicker saturable absorber or a higher concentration saturable absorber. From Fig. 5(a), the Q-switched pulse energy decreases dramatically when the reflectivity of output coupler is high, especially when the reflectivity is close to unity, because the output energy relates directly to the amount of the output coupling. With different concentration of Cr^{4+} :YAG saturable absorber, the higher the concentration of saturable absorber or the thicker the saturable absorber, the higher the pulse energy obtained. The pulse energy nearly keeps the constant when the reflectivity is in the range from 50% to 70% for a specific concentration of the saturable absorber. As indicated in Fig. 5(b), there is an optimum reflectivity of output coupler with which the shortest pulse width of Q-switched Yb:YAG lasers can be achieved. The optimum reflectivity of

output couplers are about 81%, 85% and 88% for three different concentrations from high to low of Cr:YAG saturable absorbers. The pulse width increases dramatically with the reflectivity of output coupler when the reflectivity of output coupler is close to the unity. From Fig. 5(a) and (b), parameters for the best passively Q-switched Yb:YAG laser performance such as the higher peak power can be obtained, the reflectivity of output coupler to realize the higher peak power output should be in near 70%. The Q-switched pulse repetition rate increases with the reflectivity of the output coupler, the higher the concentration of the saturable absorber, the lower the repetition rate for a certain reflectivity of the output coupler (as shown in Fig. 5(c)).

The better performance of passively Q-switched Yb:YAG laser with Cr^{4+} :YAG as saturable absorber can be achieved by using shorter laser cavity, which will result in short pulse duration, so the higher peak power output. In [4], the short laser cavity of 52 mm (Fig. 1(b)) was used and better laser performance was obtained. The passively Q-switched laser performance of laser diode pumped Yb:YAG laser was investigated in detail below. Using the parameters given in [4], such as the reflectivity of the output coupler, $R = 85\%$, the cavity length is 52 mm, the intracavity loss is estimated to be 8%, the initial ground state population density, $N_{s0} = 4.12 \times 10^{17} \text{ cm}^{-3}$, and length of the saturable absorber is 0.85 mm. The coupled rate equations Eqs. (1)–(3) were solved numerically, Fig. 6 shows the numerical simulation of the passively Q-switched laser including pulse energy, pulse width and repetition rate as functions of pump rate. From Fig. 6, we can see that the numerical results are in good agreement with the experimental results. Good laser performance of passively Q-switched Yb:YAG lasers with Cr^{4+} :YAG as saturable absorber can be achieved by using high concentration Cr^{4+} :YAG or thicker Cr^{4+} :YAG saturable absorber, higher pump rate and shorter laser cavity with an optimum reflectivity of the output coupler. For this kind of laser cavity design, the second-harmonic generation can be easily realized by insert a certain second-harmonic generation crystal inside the laser cavity. These numerical simulation of laser performance

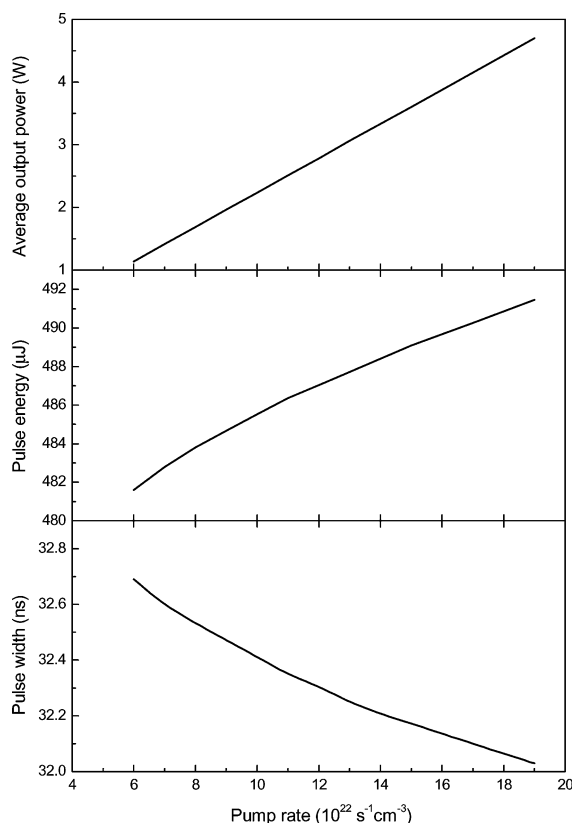


Fig. 6. The output characteristics of passively Q-switched Yb:YAG laser performance as a function of pump rate with short laser cavity.

of passively Q-switched Yb:YAG lasers with Cr^{4+} :YAG as saturable absorber and experimental results can be a good guideline for developing high power output passively Q-switched microchip Yb:YAG lasers or the second-harmonic laser output of such microchip lasers.

4. Conclusions

The passively Q-switched Yb:YAG lasers with Cr^{4+} :YAG as saturable absorber were investigated in theory. The modified coupled rate equations including the pump term and the excited state absorption of the saturable absorber of passively Q-switched Yb:YAG lasers with Cr^{4+} :YAG as saturable absorber are solved numerically. The characteristics of the passively Q-switched laser

output as functions of the initial population of the ground state of the Cr^{4+} :YAG saturable absorber, the pump rate, the reflectivity of the output coupler and the cavity length are studied in details. The simulation results show that the results obtained numerically are in good agreement with those obtained experimentally. The better laser performance can be achieved by using high concentration or thicker saturable absorber, higher pump rate and shorter laser cavity with an optimum reflectivity of the output coupler. A typical passively Q-switched laser pulse of 0.49 mJ with 32 ns in width at the repetition rate of 17 kHz can be obtained with a typical laser configuration (Fig. 1 (b)), which results in 15.3 kW peak power.

References

- [1] J.A. Morris, C.R. Pollock, *Opt. Lett.* 15 (1990) 440.
- [2] Y. Shimony, Z. Burshtein, A. Ben-Amar Baranga, Y. Kalisky, M. Strauss, *IEEE J. Quantum Electron.* 32 (1996) 305.
- [3] J. Dong, P. Deng, Y. Liu, Y. Zhang, J. Xu, W. Chen, X. Xie, *Appl. Opt.* 40 (24) (2001) 4303.
- [4] Y. Kalisky, C. Labbe, K. Waichman, L. Kravchik, U. Rachum, P. Deng, J. Xu, J. Dong, W. Chen, *Opt. Mater.* 19 (4) (2002) 403.
- [5] D.S. Sumida, T.Y. Fan, *Opt. Lett.* 19 (1994) 1343.
- [6] T.Y. Fan, *IEEE J. Quantum Electron.* 29 (1993) 1457.
- [7] S.L. Yellin, A.H. Shepard, R.J. Dalby, J.A. Baumaum, H.B. Serreze, T.S. Guide, R. Solarz, K.J. Bystrom, C.M. Harding, R.G. Walters, *IEEE J. Quantum Electron.* 29 (1993) 2058.
- [8] H.W. Bruesselbach, D.S. Sumida, R.A. Reeder, R.W. Byren, *IEEE J. Sel. Top. Quant. Electron.* 3 (1997) 105.
- [9] T.Y. Fan, S. Klunk, G. Henein, *Opt. Lett.* 18 (1993) 423.
- [10] G.J. Spuhler, R. Paschotta, M.P. Kullberg, M. Graf, M. Moser, E. Mix, G. Huber, C. Harder, U. Keller, *Appl. Phys. B* 72 (2001) 285.
- [11] A.E. Siegman, *Lasers*, University Sciences, Mill Valley, CA, 1986.
- [12] J.J. Degnan, *IEEE J. Quantum Electron.* 31 (11) (1995) 1890.
- [13] X. Zhang, S. Zhao, Q. Wang, Q. Zhang, L. Sun, S. Zhang, *IEEE J. Quantum Electron.* 33 (12) (1997) 2286.
- [14] G. Xiao, M. Bass, *IEEE J. Quantum Electron.* 33 (1) (1997) 41.
- [15] F.D. Patel, R.J. Beach, *IEEE J. Quantum Electron.* 37 (5) (2001) 707.
- [16] J.J. Degnan, *IEEE J. Quantum Electron.* 25 (1989) 214.
- [17] W. Kochner, *Solid State Laser Engineering*, fourth ed., Springer, Berlin, 1996, pp. 452.